Emission regimes in a distributed feedback tapered master-oscillator power-amplifier at 1.5 μm

M. Vilera, J. M. G. Tijero, A. Consoli, S. Aguilera, P. Adamiec, I. Esquivias

ABSTRACT

Integrated master-oscillator power amplifiers driven under steady-state injection conditions are known to show a complex dynamics resulting in a variety of emission regimes. We present experimental results on the emission characteristics of a 1.5 μm distributed feedback tapered master-oscillator power-amplifier in a wide range of steady-state injection conditions, showing different dynamic behaviors. The study combines the optical and radio-frequency spectra recorded under different levels of injected current into the master oscillator and the power amplifier sections. Under low injection current of the master oscillator the correlation between the optical and radio-frequency spectral maps allows to identify operation regimes in which the device emission arises from either the master oscillator mode or from the compound cavity modes allowed by the residual reflectance of the amplifier front facet. The quasi-periodic occurrence of these emission regimes as a function of the amplifier current is interpreted in terms of a thermally tuned competition between the modes of the master oscillator and the compound cavity modes. Under high injection current of the master-oscillator, two different regimes alternate quasi-periodically as a function of the injected current in the power amplifier: a stable regime with a single mode emission at the master oscillator frequency, and an unstable and complex self-pulsating regime showing strong peaks in the radio-frequency spectra as well as multiple frequencies in the optical spectra.

Keywords: semiconductor lasers, laser dynamics, MOPA, self-pulsation.

1. INTRODUCTION

A good number of potential diode laser applications require high power, beam quality and single longitudinal mode operation. The tapered Master Oscillator Power Amplifier (MOPA) architecture is a suitable choice for these applications. Monolithically integrated MOPAs are two sections devices, an index guided single lateral mode waveguide section acting as a master oscillator (MO), and a Power Amplifier (PA) section. The master oscillator is either a Distributed Bragg Reflector (DBR) or a Distributed Feedback (DFB) laser, while the power amplifier is a flared section with antireflection coated output facet. In the ideal performance of these devices the single lateral and longitudinal mode generated by the oscillator is launched into the amplifier section where it undergoes free diffraction and amplification while keeping its initial beam quality.

In the last years, a good deal of progress has been achieved in the development of monolithically integrated MOPA sources. 12 W output power in continuous-wave (CW) regime has been demonstrated at 1064 nm as well as pulse generation with 42 W peak power and 84 ps pulse width [1]. At an eye-safe wavelength close to 1.5 μm, commercial devices achieve 1.6 W output power in CW conditions and recently we have demonstrated the generation of 100 ps wide pulses with peak power up to 2.7 W at 1 GHz by Gain-Switching (GS) the MO section of these devices [2]. However, the obvious advantages of integrated MOPAs in comparison with their hybrid versions in terms of compactness and integrability can be jeopardized by the appearance of multiple emission instabilities even when both sections are driven in CW conditions [2-8]. Many of these instabilities are related with the appearance of modes of the whole MOPA cavity acting as a compound cavity due to the residual reflectance of the amplifier front facet that allows optical feedback. Interaction and competition between these modes and with the MO mode results in ripples in the Power-Current characteristics [2,3, 6-8] and self-pulsations caused by the mode beating at the frequency of the spacing between neighboring modes in the optical spectra [2-3].

In our previous works [2, 3], we have analyzed the CW emission characteristics of a monolithic MOPA emitting at 1.5 μm under specific injection conditions in the neighborhood of a ripple of the P-I characteristics at low injection conditions of the MO section. In this work we present a more extend and detailed experimental study of the mode competition and hopping based on the analysis of the maps of the optical and RF spectra as a function of the PA injection

current for a constant injection of the MO section. We also identify self-pulsation regimes under high injection currents of the MO section.

This paper is organized as follows: the experimental techniques are briefly described in section 2; in section 3 the experimental results are presented and discussed, and the conclusions are summarized in section 4.

2. EXPERIMENTAL

The device is a commercially available MOPA with emission wavelength at 1547 nm (QPC Lasers 4715-0000). It consists of a DFB Master Oscillator and a tapered Power Amplifier. The total device length is around 2.5 mm, and its output facet width is around 250 μm. The device is p-up mounted onto a C-mount. More details about devices from this manufacturer can be found in [9].

The experimental set-up is schematically shown in Fig. 1. Two independent CW current sources supply the current to the oscillator (I_{MO}) and amplifier sections (I_{PA}). The spectral measurements were performed by collecting a fraction of the emitted light through a lensed single-mode fiber placed close to the MOPA output facet. The fraction of collected power was around 0.1% of the total. An Optical Isolator (OI) was used to reduce the back reflection from the set-up into the device. Light was split by a fiber optical coupler (10:90) and its output ports were connected to an Optical Spectrum Analyzer (OSA, Ando AQ6315 with a resolution of 0.05 nm) and to a 45 GHz photodiode (PD2, New Focus 1014) and an Electrical Spectrum Analyzer (ESA, Agilent E4446A) with 44 GHz frequency range. We checked that at the driving conditions studied, the recorded optical and RF spectra were quite similar for different positions of the fiber tip, and then for different amounts of collected power.

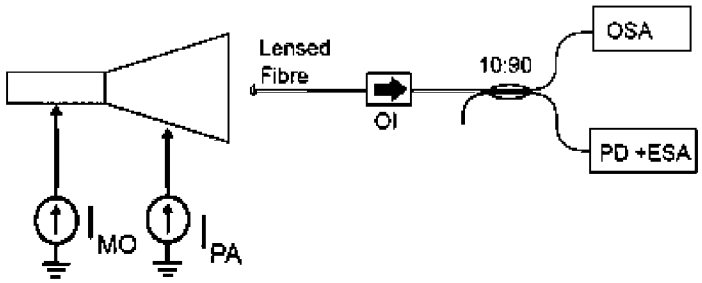

Fig. 1: Schematics of the experimental set-up. I_{MO}: Master oscillator current. I_{PA}: Power amplifier current. OI: Optical isolator. OSA: Optical spectrum analyzer. ESA: Electrical spectrum analyzer. PD: Photodiode.

The total output optical power was measured with a broad area thermal detector (Gentec UP19K-30H-H5), placed close to the MOPA output facet and slightly tilted to avoid undesired optical feedback. All measurements were performed at a constant temperature of 20°C.

3. EXPERIMENTAL RESULTS AND DISCUSSION

In the following we present separately the experimental results for two different injection regimes of the MO, low and high current injection, in which two different phenomena take place. At low injection current, we have observed periodic competition between the compound cavity modes and the DFB resonance; at medium to high injection current in the DFB section, we observed the alternation between emission regimes characterized by stable single mode emission and strong self-pulsation with multi-peak optical spectra. Fig. 2 shows the total optical power versus the amplifier current for the two selected values of the oscillator current: I_{MO} = 30 mA and I_{MO} = 300 mA. The clear appearance of ripples in the curve at low oscillator current, as well as the not so clear kinks at I_{MO} = 300 mA, are correlated with different spectral behaviors as it is described in following paragraphs.

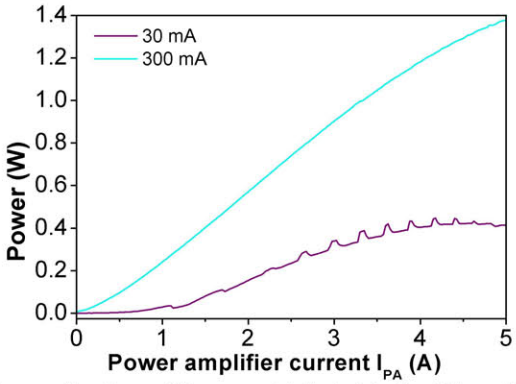

Fig. 2: Output power of the MOPA as a function of the current injected in the PA section for a constant current injected in the MO section, I_{MO} = 30 mA and I_{MO} = 300 mA.

3.1 Low injection of the Master Oscillator

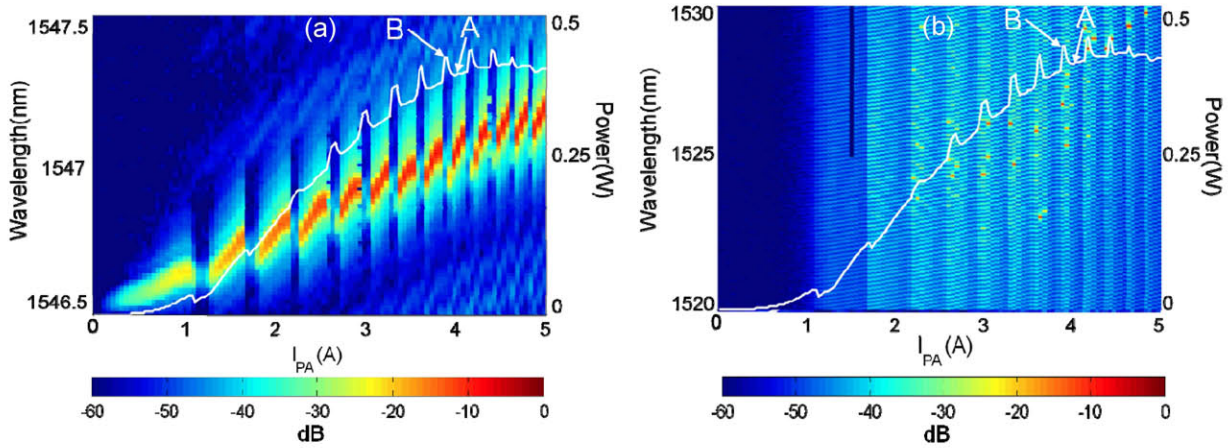

Fig. 3: Color map of the optical spectra of the MOPA as a function of I_{PA} for I_{MO} = 30 mA. The map is shown in two spectral regions, 1546.5 - 1547.5 nm (a) and 1520 – 1530 nm (b). The P-I_{PA} curves have been superimposed for reference. The intensity has been normalized to the maximum intensity in the whole map and plotted in a logarithmic color grading. The black vertical line at about I_{PA}=1.5A in (b) is an artifact.

Figure 3 shows a color map of the spectral distribution of the optical power in the entire range of I_{PA}, for I_{MO} = 30 mA. The intensity has been normalized to the maximum intensity in the whole map and has been plotted in a logarithmic color grading. The spectral region of the main laser peak is plotted in Fig 3(a) and the spectral region 1520 - 1530 nm is plotted in Fig 3(b), in a different wavelength scale. The P-I_{PA} characteristic (total optical power) has been superimposed on each plot for reference. Vertical fringes with sharp edges are apparent in both maps. The edges of each fringe are coincident in both spectral regions with the rise and the fall of a ripple in the P-I_{PA} curve. In each fringe, an anti-correlation between the optical power in each spectral region is also clearly seen. It is clear that there are two different emission regimes with a quasi-periodicity with the amplifier current: multi-mode emission at around 1525 nm, corresponding to the peaks of the power-current ripples, and single mode emission at around 1547 nm, corresponding to the valleys. Figs. 4a and 4b show, respectively, the optical spectra at the bias conditions of the points labeled as A and B in Fig. 3, respectively, which correspond to the two different regimes.

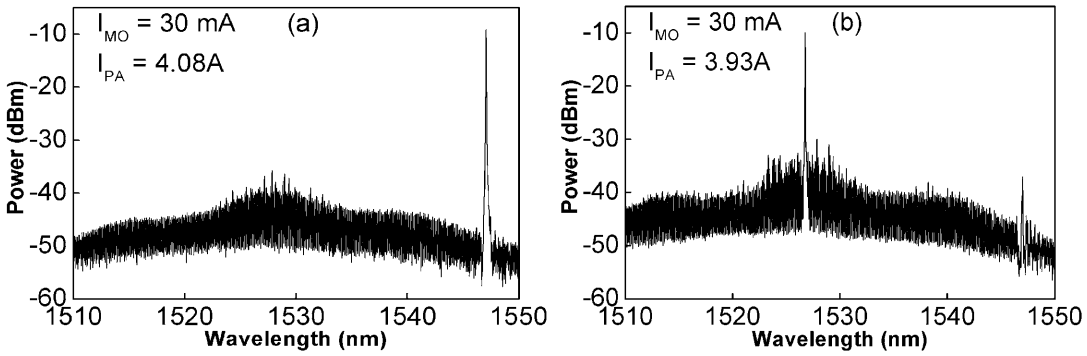

Fig. 4: Logarithmic plot of the optical spectra of the MOPA under injection conditions A (a) and B (b).

Under conditions A, almost all the power of the device is emitted in the DFB mode at about 1547 nm, whereas the maximum Amplified Spontaneous Emission (ASE) appears around 1527 nm. Under conditions B the situation is quite the opposite. In this case the emission wavelength is at the maximum of the ASE spectra as in conventional Fabry-Perot lasers. The distance between ASE peaks is 0.14 nm, which corresponds to the total cavity length of 2.5 mm.

In line with previous reports on 980 nm MOPAs [6-8], our qualitative interpretation of this behavior is as follows: At injection conditions A-like the lasing takes place at the wavelength selected by the design of the DFB grating and the device behaves as expected from a MOPA: the laser emission generated in the MO section undergoes amplification in the PA section without spectral changes. As I_{PA} increases, the heat generated in the amplifier section slightly increases the temperature of the MO section and therefore, the spectral position of the Bragg condition shifts to a higher wavelength due to the thermal increase of its refractive index. The mode competition between the compound cavity modes in the region of high material gain and the Bragg region results in the prevalence of the latter. However, a further increase of I_{PA} eventually shifts the phase of the active feedback of the amplifier section, reducing the gain at the DFB emission region and producing lasing in the region of the maximum amplifier gain. This value of I_{PA} marks the edge of the fringe in both spectral regions. For higher values of I_{PA} the spectra results in a B-like fringe. Now the compound cavity works as a laser emitting in a mode in the high material gain region (1520 -1535 nm) (Fig. 3b). The emission at about 1547 nm is virtually absent while the comb of ASE peaks of the compound cavity becomes brighter in the region 1520 - 1535 nm. It is worth to point out that the active mode hopping in these conditions results in a seeming distribution of the optical power among several modes, such that none of them seems to have the power lacking in the 1547 nm region. This is obviously only a consequence of the fast dynamics of mode hopping in comparison with the slow process of recording the spectra. A further increase of I_{PA} eventually leads to the required temperature increase of the MO section and of the amplifier section to provide the lasing conditions at a slightly shifted wavelength position in the Bragg grating region.

Fig. 5a shows the map of the measured RF spectra sweeping the amplifier current. The P-I_{PA} characteristic has been also plotted for reference. The RF spectra at the previous bias conditions A and B are shown in Fig. 5b. The correlation of the RF and optical spectra with the two emission regimes can be clearly understood as follows: in the single mode emission regime, there is no apparent RF peak, except the relatively low frequency contribution of the Relative Intensity Noise at 2- 3 GHz; in the multimode emission regime, the beating of the Fabry-Perot modes of the complete cavity produces the self-pulsation peak at 18 GHz (~0.14 nm) and the corresponding high order harmonics.

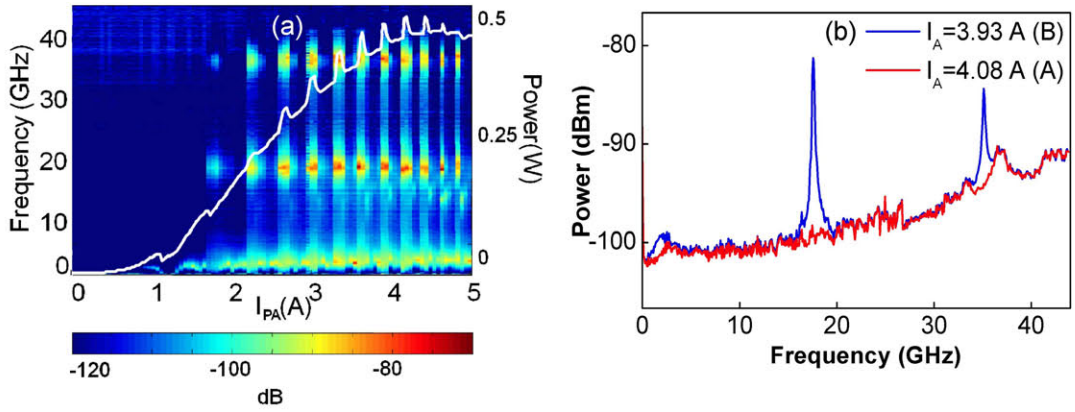

Fig. 5: (a) Color map of the RF spectra of the MOPA as a function of I_{PA} for I_{MO} = 30 mA. The RF power is plotted in relative units in a logarithmic color grading. The P-I_{PA} curve has been superimposed for reference. (b) Logarithmic plot of RF spectra under injection conditions A and B.

3.2 High injection of the Master Oscillator

At high injection current of the master oscillator the device behaves quite differently. Fig. 6 shows a color map of the optical spectra recorded as a function of I_{PA} for a constant current in the master oscillator I_{MO}=300 mA. The intensity has been normalized to the maximum intensity in the whole map. The total power emitted under these conditions is plotted in the P-I curve of Fig. 2 above. Under these conditions, no significant power is emitted in the spectral region of the maximum (1520-1530 nm) revealing the prevalence of the modes in the master oscillator region for the entire range of conditions. The continuous red shift of the laser peak interrupted by sudden and quasi-periodic drops of the peak wavelength can be attributed, in line with Spreemann [7], to a cross-heating effect by which the heat generated in the PA section increases the temperature of the MO section and tunes quasi-periodically the resonant mode as described above.

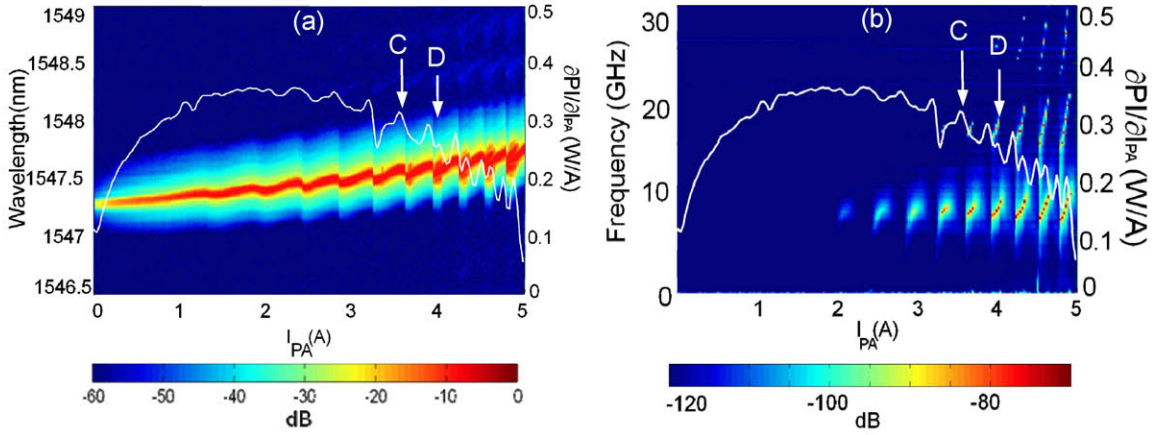

Fig. 6: Color map of the optical spectra in the region [1546.5 – 1547.5] nm (a) and color map of the RF spectra of the MOPA (b) as a function of I_{PA} for I_{MO}=300 mA. The first derivative of the power-amplifier current P-I_{PA} has been superimposed for reference. The intensity has been normalized to the maximum intensity in the whole map and plotted in a logarithmic color grading.

At high I_{PA}, a closer look into the spectra plotted in Fig. 6 reveals that in each period between 2 drops the laser peak broadens for a range of injection conditions close to the drops. These spectral features are not apparent in the P-I_{PA} curve (fig. 2), however they manifest as undulations in its derivative, each undulation marking the border between either the conditions for a drop of the laser wavelength or the borders between narrow and broad laser peaks (see Fig. 6).

Significant insight into the characteristics of the emitted light in each region can be gained by plotting the RF spectra. Fig 6b is a color map of these RF spectra recorded simultaneously to the optical spectra plotted in Fig. 6.a.

A comparative look at Figs 6a and 6b (helped by the derivative of the P-I curve) reveals that as I_{PA} increases a regime with stable CW emission and narrow optical spectrum alternates with an unstable regime characterized by a broader optical spectrum and an RF peak at about 8 GHz with higher order harmonics which are more clearly seen at high I_{PA}.

In order to examine locally the details of these two regimes the optical and RF spectra have been recorder under typical conditions for each regime. These conditions are indicated in Fig. 6 and 7 as C (I_{PA}=3.6A) (stable) and D (I_{PA}=4A) (unstable). Fig. 7a and 7b show respectively the optical and RF spectra recorded under conditions C and D. The width of the optical peak under conditions C is limited by the resolution of the spectrum analyzer whereas the peak at D is broadened by side peaks separated by 0.06 nm with respect to the main peak. Consistent with stable CW emission the RF spectrum at C shows no significant feature while a strong fundamental peak at 7.6 GHz and three harmonics are clearly visible in the spectrum at D indicating a self-pulsating regime. The 0.06 nm separation between the side peaks and the main peak in the optical spectrum at D corresponds with the frequency of the RF peak but is much lower than the separation between the Fabry-Perot modes of the passive compound cavity (0.14 nm).

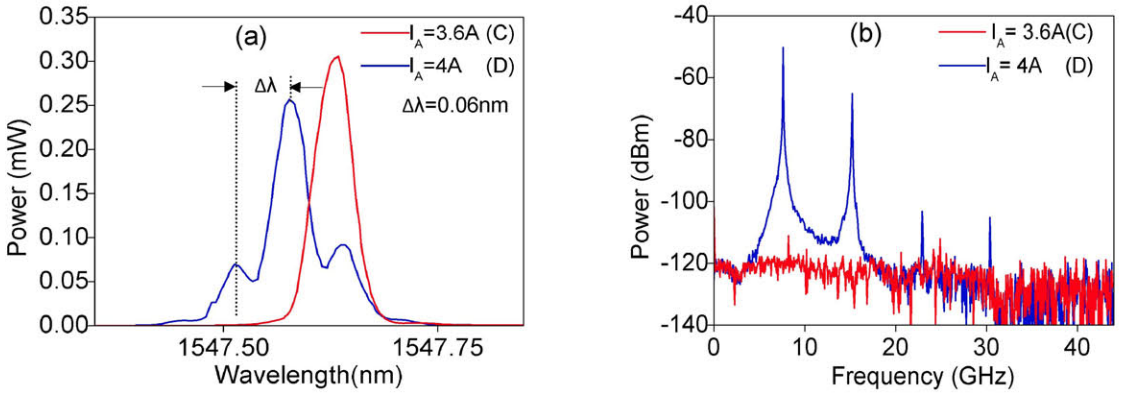

Fig. 7: Lineal plot of the optical spectra (a) and logarithmic plot of RF spectra (b) of the MOPA under injection conditions C and D.

Similar sequences of stable and unstable self-pulsating regimes have been experimentally observed and theoretically analyzed in devices specifically designed to have a separate control of the phase and the intensity of the optical feed-back [10-12]. In our case, the tuning of both, phase and intensity, by increasing the power amplifier current is expected to give rise to a complex sequence of the stable CW regime followed by different kind of pulsating regimes.

4. CONCLUSIONS

The dynamics of an integrated MOPA at 1.55 mm under CW injection conditions has been experimentally studied. Stable and unstable regimes have been identified under both low and high injection of the master oscillator. Under low injection of the master oscillator the stable regime alternates with a self-pulsing regimen at 18 GHz. The origin of this pulsation is the beating of compound cavity Fabry-Perot modes of frequencies close to the maximum of the ASE spectrum and therefore its peak wavelength is shifted by about 20 nm with respect to the lasing wavelength in the stable regime. Under high injection of the master oscillator the stable regime alternates with a more complex self-pulsing regime at frequencies around 8 GHz. In this unstable regime the MOPA emits in the same spectral region but the laser peak broadens with side peaks separated from the main peak by about 0.06 nm in correspondence with the pulsation frequency. Besides the continuous thermal red shift the wavelength of the laser peak undergoes quasi-periodic drops attributed to thermal tuning of the refractive index profile in the master oscillator.

ACKNOWLEDGMENT

This work was supported by the European Commission through the project BRITESPACE under grant agreement Nº. 313200 and by Ministerio de Economía y Competitividad of Spain under project TEC2012-38864-C03-02.

5. REFERENCES

[1] Wenzel, H., Schwertfeger, S., Klehr, A., Jedrzejczyk, D., Hoffmann, T., and Erbert, G., "High peak power optical pulses generated with a monolithic master-oscillator power amplifier," Opt. Lett. 37(11), 1826-1828 (2012).

[2] Adamiec, P., Bonilla, B., Consoli, A., Tijero, J.M.G., Aguilera, S., and Esquivias, I., "High-peak-power pulse generation from a monolithic master oscillator power amplifier at 1.5 μm," Appl. Opt. 51(30), 7160-7164 (2012).

[3] Adamiec, P., Bonilla, B., Consoli A., Tijero, J.M.G., Aguilera, S., Esquivias, I., Vilera, M., Javaloyes, J. and Balle, S., "Dynamic response of a monolithic master-oscillator power-amplifier at 1.5 μm." Proc. SPIE 8640, Novel In-Plane Semiconductor Lasers XII, 86401M (March 4, 2013); doi:10.1117/12.2004366

[4] Wright, M.W. and Bossert, D.J. "Temporal dynamics and facet coating requirements of monolithic MOPA semiconductor lasers," IEEE Photon. Technol. Lett. 10, 504-506 (1998).

[5] Egan A., Ning, C.Z., Moloney, J.V., Indik, R.A., Wright, M.W., Bossert, D.J. and J.G. McInerney, "Dynamic instabilities in master oscillator power amplifier semiconductor lasers," IEEE J. Quantum Electron. 34, 166-170 (1998).

[6] Radziunas, M., Tronciu, V.Z., Bandelow, U., Lichtner, M., Spreeman, M., Wenzel, H., "Mode transitions in distributed-feedback tapered master-oscillator power amplifier: theory and experiments," Opt. Quant. Electron. 40, 1103-1109 (2008).

[7] Spreemann, M., Lichtner, M., Radziunas, M., Bandelow, U. and Wenzel, H., "Measurement and Simulation of Distributted-feadback tapered master-oscillator power-amplifiers," IEEE J. Quantum Electron. 45, 609-616 (2009).

[8] Tronciu, V.Z., Lichtner, M., Radziunas, M., Bandelow, U., and Wenzel, H., "Improving the stability of distributed-feedback tapered master-oscillator power-amplifiers," Opt. Quantum Electron. 41, 531-537 (2009)

[9] Osowski, M.L., Gewirtz, Y., Lammert, R.M., Oh, S.W., Panja, C., Elrade, V.C., Vaissié, L., Patel, F.D. and Ungar, J.E., "High-power semiconductor lasers at eye-safe wavelengths," Proc. SPIE 7325, 7325-29 (2009).

[10] Phelan P., McDonald D., Egan A., Hegarty J., O'Dowd R., Farrell G. and Lindgren S., "Comparison of self-pulsation in multisection lasers with distributed feedback and intracavity saturable absorbers," IEE Proc. Optoelectronics 141(2) (1994).

[11] Bauer S., Brox O., Kreissl J., Sartorius B., Radiuznas M. and Sieber J. "Nonlinear dynamics of semiconductor lasers with active optical feedback," Phys. Rev. E, 69, 016206 (2004).

[12] Heil. T., Fisher I., Elsäber. W., Krauskopf B., Grren K. and Gavrielides A., "Delay dynamics of semiconductor lasers with short external cavities: Bifurcation scenarios and mechanisms," Phys. Rev. E, 67, 066214 (2003).